Product user guide – Microwave FCDR release 4.1

Imke Hans, Martin Burgdorf and Emma Woolliams

University of Hamburg and National Physical Laboratory

1/29/2019

FIDUCEO has received funding from the European Union's Horizon 2020 Programme for Research and Innovation, under Grant Agreement no. 638822

1 Contents

2 Introduction

2.1 Scope

This document describes the Microwave "easy" FCDR data files of version 4.1 uploaded to CEDA in January 2019. The released data record contains all mission years of SSMT2 on F11, F12, F14, F15, AMSU-B on NOAA15, NOAA16 and NOAA17 and MHS missions (NOAA18, NOAA19, MetopA,-B), i.e. a data record long enough to generate climate data records (CDRs) for climate research. The presented FCDR is a long data record of increased consistency among the instruments compared to the operational data record. The improvements are based on the strict application of the measurement equation as well as dedicated corrections and improvements within the calibration process. The data record is uncertainty quantified, respecting the correlation behaviour of underlying effects. This product user guide gives:

1. An overview of the specifications of the data record;
2. Scientific records on the generation, definition, and algorithms of the data record;
3. Information on limitations of this version of the data record;
4. Technical details on the format and on how to access the data.

2.2 Version Control

Version	Reason	Reviewer	Date of Issue
0.1	Initial version		
0.2	Second version		7. March 2018
0.3	Third version		16. October 2018
4.1	Fourth version		Release for final FIDUCEO FCDR (version number matches FCDR version)

2.3 Applicable and Reference Documents

- FIDUCEO website, http://www.fiduceo.eu/
- D2-2, Report on the MW FCDR: Uncertainty (contact fiduceo-coordinator@lists.reading.ac.uk)
- D2-2a, Principles of FCDR Effects Tables (contact fiduceo-coordinator@lists.reading.ac.uk)
- CF-standards version 1.7, http://cfconventions.org/Data/cf-conventions/cf-conventions-1.7/cf-conventions.html
- [Hans et al 2017]: Hans, I., Burgdorf, M., John, V. O., Mittaz, J., and Buehler, S. A.: Noise performance of microwave humidity sounders over their lifetime, Atmos. Meas. Tech., 10, 4927-4945, https://doi.org/10.5194/amt-10-4927-2017, 2017.
- [Atkinson 2001]: Atkinson, N. C.: Calibration, monitoring and validation of AMSUB, Adv. Space Res., 28, 117–126, https://doi.org/10.1016/S0273- 1177(01)00312-X, 2001
- [Atkinson 2000]: Atkinson, N.: Performance of AMSU-B Flight Model 2 (FM2) during NOAA-L Post Launch Orbital Verification Tests; Document Reference No: AMB112; MetOffice, November 2000

- [Atkinson 2002]: Atkinson, N.: Performance of AMSU-B Flight Model 3 (FM3) during NOAA-M Post Launch Orbital Verification Tests; Document Reference No: AMB113; MetOffice, September 2002
- [John 2013a]: John, V. O., R. P. Allan, W. Bell, S. A. Buehler, and A. Kottayil (2013), Assessment of intercalibration methods for satellite microwave humidity sounders, J. Geophys. Res. Atmos., 118, doi:10.1002/jgrd.50358.
- [John 2013b]: John, V. O., G. Holl, N. Atkinson, and S. A. Buehler (2013), Monitoring scan asymmetry of microwave humidity sounding channels using simultaneous all angle collocations (SAACs), J. Geophys. Res. Atmos., 118, 1536–1545, doi:10.1002/jgrd.50154
- [Hans 2018]: Hans, I.: Towards a new fundamental climate data record of microwave humidity sounders based on metrological best practice, Doctoral thesis, 2018, Universitaet Hamburg
- [Hans et al 2019a]: Hans, I. Burgdorf, M., Buehler, S.A., Lang, T., Prange, M., John, V.O.: An uncertainty quantified fundamental climate data record for microwave humidity sounders, in preparation for special issue on climate data records in Remote Sensing
- [Hans et al 2019b]: Hans, I. Burgdorf, M., Buehler, S.A.: On-board radio frequency interference as origin of inter-satellite biases for microwave humidity sounders, in preparation for special issue on Radio Frequency Interference in Remote Sensing

2.4 Glossary

AAPP	ATOVS and AVHRR Pre-processing Package
AMSU-B	Advanced Microwave Sounding Unit –B
BT	Brightness Temperature
CEDA	Centre for Environmental Data Archiving
CF	Climate and Forecast
CLASS	Comprehensive Large-Array Stewardship System
CPIDS	Calibration Parameters Instrument Data Set
DSV	Deep space view
EUMETSAT	European Organisation for the Exploitation of Meteorological Satellites
FCDR	Fundamental Climate Data Record
FIDUCEO	Fidelity and Uncertainty in Climate data records for Earth Observation
FOV	Field Of View
FTP	File Transfer Protocol
IASI	Infrared Atmospheric Sounding Interferometer
ICCT	Internal Cold Calibration Target
IWCT	Internal Warm Calibration Target
MHS	Microwave Humidity Sounder
NCC	National Calibration Center
NESDIS	National Environmental Satellite, Data, and Information Service
NOAA	National Oceanic and Atmospheric Administration
PRT	Platinum Resistance Thermometer
RFI	Radio Frequency Interference
SARR-A/-B	Search and Rescue Repeater A and B
SNO	Simultaneous Nadir Overpass
SRF	Spectral Response Function
STAR	Center for Satellite Applications and Research
STX1-4	S-band transmitter 1-4

3 FCDR overview characteristics

General	FCDR name	FIDUCEO FCDR Microwave Brightness Temperatures with uncertainties
	FCDR reference	Paper in preparation for Remote Sensing Special Issue (Feb 2019) [Hans et al 2019a]: „An uncertainty quantified fundamental climate data record for microwave humidity sounders“
	FCDR digital identifier(s)	doi:10.5285/ 8e9f44965434f3b861eba77688701ef
	FCDR description	Recalibrated brightness temperatures for Microwave radiometers AMSU-B and MHS, with uncertainty estimates on pixel level, with correlation length scales estimates. Harmonised version (corrected calibration).
	FCDR type	Microwave sounder FCDR
	FCDR period	encompasses all years between 1994-2017
	FCDR satellites	• F11 • F12 • F14 • F15 • NOAA-15 • NOAA-16 • NOAA-17 • NOAA-18 • NOAA-19 • MetOp-A • MetOp-B
	FCDR content	Brightness temperatures and uncertainties generated with MATLAB code
Instrument	Instrument name	Advanced Microwave Sounding Unit-B (AMSU-B), Microwave Humidity Sounder (MHS), Special Sensor Microwave Water Vapor Profiler (SSMT-2)
	Instrument description	AMSU-B, MHS and SSMT-2 are scanning radiometers. They scan the Earth in 90 Earth views (28 for SSMT-2) per scan line in five spectral channels. An overview of the channels is given later. For every scan line, the instrument gets a new calibration based on 4 views of a warm target and 4 views of a cold target.

Data	Input data	• input data are L1B data files obtained from the NOAA CLASS archive • some calibration parameters are obtained from the fdf.dat and mhs_clparams.dat/ amsub_clparams.dat file of the AAPP, most of them also appear in the l1b data header and are read from there • auxiliary log-files produced with AAPP subroutine amsubcl/mhscl per L1B file (needed to perform moon-intrusion-check)
	Output data	Microwave "easy" FCDR including brightness temperatures and uncertainties split into independent, structured and common components Each MW Easy FCDR file of this version contains: • Basic telemetry: longitude, latitude, time, satellite and solar angles (these angles are not provided for SSMT-2); • Brightness temperatures for channels 1-5; • Independent, structured and common uncertainty for channels 1-5; • for each scan line: original scan line number of the l1b files • for each scan line: indicator which l1b file it belongs to • 8 bitfields indicating identified problems with the data: one bitmask indicating level of trust in the data (per pixel and scanline), one bitmaks indicating sensor specific quality issues (per pixel and scanline); one bitmask indicating quality issues per scan line, i.e. transmitter status so far (per scanline), 5 bitmasks indicating certain quality issues for each channel (per pixel and per scanline) The dimensions of the variables in the NetCDF file are x and y, indicating the pixel and scan line, respectively. Additionally, there are the dimensions channel and n_frequencies, denoting the number of channels and the number of frequencies (for which Spectral Response Function is defined).
	Format	The data are provided in NetCDF4 format.
Access	CEDA	The data are hosted by CEDA. This version for MW will be in the format /AMSUB/v4.1/ SATELLITE/YEAR/MONTH/DAY /MHS/v4.1/ SATELLITE/YEAR/MONTH/DAY /SSMT2/v4.1/ SATELLITE/YEAR/MONTH/DAY
	Delivery	Available through CEDA
Resolutio	Horizontal	Footprint size corresponds to a circle of about 16 km diameter at nadir for AMSU-B and MHS.

	Vertical	Surface and sounding channels (troposphere), resolution depends on atmospheric state
	Temporal	Polar-orbiting; most places seen at least daily but less frequently at same angle
Physical Content	FCDR physical quantity	The core physical quantity consists of Planck Brightness Temperatures for each channel for each Earth view. Associated information stored in the same files is latitudes, longitudes, independent uncertainties, structured uncertainties and common uncertainties.
	FCDR physical description	One “easy “ FCDR orbit-file is about 7 MB. For the normal case, one file contains one full orbit from (ascending/descending) equator crossing to the next (ascending/descending) equator crossing of the nadir views.
Uncertainty target	Accuracy	Metrologically traceable uncertainties provided for each measurement.
	Precision	BTs and their uncertainties are stored with a precision of 0.01K.
	Stability	The instruments agree within their uncertainties due to common effects. They agree within about 0.25 K for 183 ±1GHz, 0.5 K for 183 ±3GHz and for 183 ±7GHz/ 190 GHz (except for NOAA-15, which has a larger bias) and about 1 K for 89 GHz and 157 GHz, note that AMSU-B and SSMT2 measure at 150 GHz, thus a larger bias than 1 K remains naturally. Note that these numbers originate from global monthly means. The good agreement results in consistent time series without major jumps. Note that some satellites drift, which may introduce diurnal cycle aliasing.
	Known problems	As there is no information on the antenna pattern correction from SSMT2, the FCDR can only contain antenna temperatures instead of brightness temperatures for SSMT2. This should be kept in mind when using the data.

Data record characteristics	The independent uncertainty describes the uncertainty in the brightness temperature due to purely random effects that generate a completely independent uncertainty from pixel to pixel. These independent effects are the noise on the Earth view counts and the random fluctuations of the angle of the Earth view. The structured uncertainties encompass effects that have a correlation scale below the time/ space scales of one orbit. The common uncertainties represent effects that have a correlation scale larger than one orbit. Usually the underlying parameters of the effect are constant over the mission.

4 Description of AMSUB and MHS

SSMT-2, AMSU-B and MHS are a passive microwave radiometer with five channels measuring in the microwave spectrum.

Instrument	Satellite	Start	End
SSMT-2	DMSP F11	1991-11-28	2000-08-07
SSMT-2	DMSP F12	1994-08-29	2008-10-13
SSMT-2	DMSP F14	1997-04-04	2015
SSMT-2	DMSP F15	1999-12-12	2015
AMSU-B	NOAA-15/K	1998-12-15	2011-03-28
AMSU-B	NOAA-16/L	2001-03-20	2014-06-09
AMSU-B	NOAA-17/M	2002-10-15	2013-04-10
MHS	NOAA-18/N	2005-08-30	
MHS	NOAA-19/N'	2009-06-02	
MHS	MetOp-A	2007-05-15	
MHS	MetOp-B	2013-01-29	

Note that this table corresponds to available operational data and current Microwave FCDR data availability is more limited: we only use data that is stored in the NOAA CLASS archive. This restricts the time range of available SSMT-2 data, since the required level 1b data is only available from CLASS for a restricted range.

Available FCDR data:

Instrument	Satellite	Start	End
SSMT-2	DMSP F11	1994-07-05	1995-04-02
SSMT-2	DMSP F12	1994-10-13	2001-01-08
SSMT-2	DMSP F14	1997-04-28	2005-01-10
SSMT-2	DMSP F15	2000-01-24	2005-01-02
AMSU-B	NOAA-15/K	1999-01-01	2011-03-28
AMSU-B	NOAA-16/L	2001-03-20	2014-04-30
AMSU-B	NOAA-17/M	2002-10-15	2013-04-10

MHS	NOAA-18/N	2005-08-30	2017-12-31
MHS	NOAA-19/N'	2009-11-01	2017-12-31
MHS	MetOp-A	2007-06-01	2017-12-31
MHS	MetOp-B	2013-01-29	2017-12-31

SSMT-2

Note the different numbering of the channels compared to MHS.

Channel	Wavelength [GHz]	Notes
1	183.31±3.0	
2	183.31±1.0	
3	183.31±7.0	
4	91.655±1.250	
5	150.00±1.25	

AMSU-B

Note that the AMSU-B channels are counted including the AMSU-A channels (1-15).

Channel	Wavelength [GHz]	Notes
16	89.0±0.9	
17	150.0±0.9	
18	183.31±1.0	
19	183.31±3.0	
20	183.31±7.0	

MHS

Channel	Wavelength [GHz]	Notes
1	89.0	
2	157.0	
3	183.31±1.0	
4	183.31±3.0	
5	190.31	

The FCDR of recalibrated MW brightness temperatures and metrologically traceable uncertainties corresponds to Task 4.3 in the Horizon-2020 project FIDUCEO (see http://www.fiduceo.eu).

5 Differences with existing products

The FIDUCEO MW FCDR differs from existing MW level-1c data, processed with AAPP:

- The calibration has been improved with a measurement function approach, providing consistent calibration for the MHS, AMSU-B and SSMT-2 instruments

- Operational calibration has been improved to yield a better, stable calibration (see also Section 6.5 on the explicit changes in some parameters of the measurement equation and a radio frequency (RFI) correction to improve the calibration)
- metrologically traceable uncertainties have been derived for three classes of correlation behaviour: independent, structured and common uncertainties
- new quality checks and flags are defined
- the files come as Equator-To-Equator files without overlap to adjacent ones
- The recalibrated MHS, AMSU-B and SSMT2 instruments provide stable long time series of brightness temperatures, especially around the water vapour absorption line at 183 GHz.

6 Calibration and uncertainty approach[1]

The MW FCDR is built on the measurement function, which calculates the Earth Radiance L_{E} from the Earth Count. The core of the measurement function is a two-point-calibration based on a warm and a cold reference target. The signal from the Earth is then compared to these reference signals. Accounting for all effects that impact on the true signal from Earth, the measurement function gains much complexity. In the following, we present the measurement function accounting for many identified effects (the incompleteness of these identified effects is represented by +0: knowing that there is or might be more to consider, but assuming that the impact is zero in order to keep things feasible).

The measurement function in its highest-level form, solved for the Earth Radiance is

$$L_{\mathrm{E},i} = \frac{\left(L_{\mathrm{ME},i} - g_{\mathrm{S},i} L_{\mathrm{CMB}} - g_{\mathrm{Pl},i} L_{\mathrm{Pl}}\right)}{\left(1 - g_{\mathrm{S},i} - g_{\mathrm{Pl},i}\right)} + 0 \qquad \textit{Eq 6-1}$$

where, the Earth radiance for a pixel i is calculated from the measured Earth radiance, $L_{\mathrm{ME},i}$ for that pixel and the radiance from space and the satellite platform that are observed in the side-lobes of the antenna gain pattern (AGP). L_{CMB} is the radiance of the cosmic microwave background, and L_{Pl} is the radiance of the satellite platform. For the FCDR, we follow the assumption made in the operational processing code AAPP, and assume that the reflectivity of the platform is one, i.e. that $L_{\mathrm{Pl}} = L_{\mathrm{E}}$. This might change in a later version.

The g terms represent the fraction of the sphere subtended by the Earth, space and the satellite platform when viewing pixel i, weighted by the antenna gain pattern, i.e.

$$g_{\mathrm{E},i} = \frac{\int_{\mathrm{Earth},\, i} AGP(\Omega)\,\mathrm{d}\Omega}{\int_{4\pi} AGP(\Omega)\,\mathrm{d}\Omega} = 1 - g_{\mathrm{S},i} - g_{\mathrm{Pl},i}\,, \qquad \textit{Eq 6-2}$$

$$g_{\mathrm{S},i} = \frac{\int_{\mathrm{Space},\, i} AGP(\Omega)\,\mathrm{d}\Omega}{\int_{4\pi} AGP(\Omega)\,\mathrm{d}\Omega}\,, \qquad \textit{Eq 6-3}$$

[1] This section is mostly copied from D2-2

$$g_{\mathrm{Pl},i} = \frac{\int_{\text{Platform, } i} AGP(\Omega)\,\mathrm{d}\Omega}{\int_{4\pi} AGP(\Omega)\,\mathrm{d}\Omega}, \qquad \textit{Eq 6-4}$$

where $AGP(\Omega)$ is the antenna gain pattern as a function of solid angle, and the upper integrals are over the solid angles subtended by the Earth, by space and by the satellite platform, respectively.

The measured Earth radiance, $L_{\mathrm{ME},i}$ in Eq 6-6, is given from the measured Earth counts and the instantaneous gain calculated from the calibration with the IWCT and space views, as well as corrections for nonlinearity and for polarisation effects:

$$L_{\mathrm{ME},i} = \tilde{L}_{\mathrm{MIWCT}} + \frac{\tilde{L}_{\mathrm{MIWCT}} - \tilde{L}_{\mathrm{MS}}}{\bar{C}_{\mathrm{IWCT}} - \bar{C}_{\mathrm{S}}}\left(C_{\mathrm{E},i} - \bar{C}_{\mathrm{IWCT}}\right) + \Delta L_{\mathrm{nl}} + \Delta L_{\mathrm{pol}} + 0 \qquad \textit{Eq 6-5}$$

where,

$\tilde{L}_{\mathrm{MIWCT}}$	Is the band-integrated measured radiance of the internal warm calibration target, see below
$\tilde{L}_{\mathrm{MS}}$	Is the band-integrated measured radiance of deep space, this includes contributions from other elements in the antenna side lobes, see below
$\bar{C}_{\mathrm{IWCT}}$	Is the averaged count signal when measuring the IWCT. This has been calculated as a weighted average from calibration measurements over several scanlines
$\bar{C}_{\mathrm{S}}$	Is the averaged count signal when measuring deep space. This has been calculated as a weighted average from calibration measurements over several scanlines
$C_{\mathrm{E},i}$	Is the count signal when measuring the Earth
ΔL_{nl}	Is a nonlinearity correction, see below
ΔL_{pol}	Is a polarisation correction, see below
+0	Represents the extent to which this equation form is an approximation.

The measured IWCT radiance is calculated from a modified Planck equation, as:

$$\tilde{L}_{\mathrm{MIWCT}} = L_{\mathrm{BB}}\left(\nu_{ch}, A + b\left(T_{\mathrm{IWCT}} + \delta T_{ch}\right)\right) + 0, \qquad \textit{Eq 6-6}$$

$$L_{\mathrm{BB}} = \frac{2h\nu_{ch}^3/c^2}{\left(\exp\left[h\nu_{ch}/\left(k_{\mathrm{B}}\left[A + b\left[T_{\mathrm{IWCT}} + \delta T_{ch}\right]\right]\right)\right] - 1\right)}$$

where, the fundamental constants h, c, k_{B} have their normal meaning, ν_{ch} is the effective frequency of the channel. A, b are band-correction coefficients which describe the difference between a Planck function evaluated at the centre frequency (183 GHz) and the average of the Planck functions at two frequencies above and below the centre frequency. They are $A = 0, b = 1$ for all channels except for channels 19 and 20 of AMSU-B and channel H4 of MHS. T_{IWCT} is the temperature measured by the platinum resistance thermometers (PRTs) on the IWCT (a weighted average), and δT_{ch} is a channel-dependent warm target bias correction that accounts for the contamination by radiation originating in the

shroud or local oscillator and other sources of bias. Eq 6-6 makes a number of simplifications discussed in the D2-2 document. The plus zero term accounts for these simplifications.

Analogously to the IWCT radiance, the space radiance is calculated as

$$L_{\mathrm{MS}} = L_{\mathrm{CMB,\,corr}}\left(\nu_{ch}, A + b(T_{\mathrm{CMB}} + a_3)\right) + 0 \qquad \text{Eq 6-7}$$

$$L_{\mathrm{CMB,\,corr}} = \frac{2h\nu_{ch}^3/c^2}{\exp[h\nu_{ch}/(k_B[A + b[T_{\mathrm{CMB}} + a_3]])] - 1}$$

where T_{CMB} is the brightness temperature of the cosmic microwave background and a_3 is a channel dependent correction that accounts for the contamination by radiation originating from the Earth or the platform (i.e. the satellite). This additive correction is a strong simplification, bearing in mind that the antenna gain pattern correction for the Earth views has a much more complex structure (see above). This complexity surely also applies for the deep space view. However, for this version we follow this simplification made in the AAPP code and use the provided additive corrections.

In Eq 6-6, the signals from the IWCT and space view already appear in their averaged form: The counts are averaged in a weighted rolling average over several scan lines k, thus:

$$\bar{C}_{\mathrm{IWCT}} = \sum_k w_k C_{\mathrm{IWCT},k}, \qquad \bar{C}_{\mathrm{S}} = \sum_k w_k C_{\mathrm{S},k} \ . \qquad \text{Eq 6-8}$$

The nominal number of averaged scan lines is 7. In a later version, this is refined for adequate handling of bad data lines.

The non-linearity correction is given by:

$$\Delta L_{\mathrm{nl}} = a_1 \frac{\left(C_{\mathrm{E},i} - \bar{C}_{\mathrm{S}}\right)\left(C_{\mathrm{E},i} - \bar{C}_{\mathrm{IWCT}}\right)}{\left(\bar{C}_{\mathrm{IWCT}} - \bar{C}_{\mathrm{S}}\right)^2}\left(\tilde{L}_{\mathrm{MIWCT}} - \tilde{L}_{\mathrm{MS}}\right)^2 \qquad \text{Eq 6-9}$$

Where a_1 is the nonlinearity coefficient and other terms have the same meaning as given above. The nonlinearity coefficient determined through pre-flight calibration is only significant for channel 1; the term is considered suitable for harmonisation for channel 1.

The polarisation correction is given by

$$\Delta L_{\mathrm{pol}} = a_2\left(\tilde{L}_{\mathrm{MIWCT}} - \hat{L}_{\mathrm{ME},i}\right)\left(\cos\left(2\vartheta_{\mathrm{E},i}\right) - \cos\left(2\vartheta_{\mathrm{S}}\right)\right)/2 + 0 \qquad \text{Eq 6-10}$$

Where, a_2, a property of the mirror is one minus the ratio of reflectivity at 90° and at nadir. The angles $\vartheta_{\mathrm{E},i}, \vartheta_{\mathrm{S}}$ are the antenna angles for the *i*th Earth view pixel and the space view pixel, respectively and $\hat{L}_{\mathrm{E},i}$ is the uncorrected Earth view radiance and the + 0 represents the extent to which this equation is an approximation.

The calibration is executed for every scan line, i.e. every 8/3 seconds.

6.1 Measurement Function Diagram

Figure 1 illustrates the measurement function diagram for the MW instruments, with the sources of uncertainty at the end.

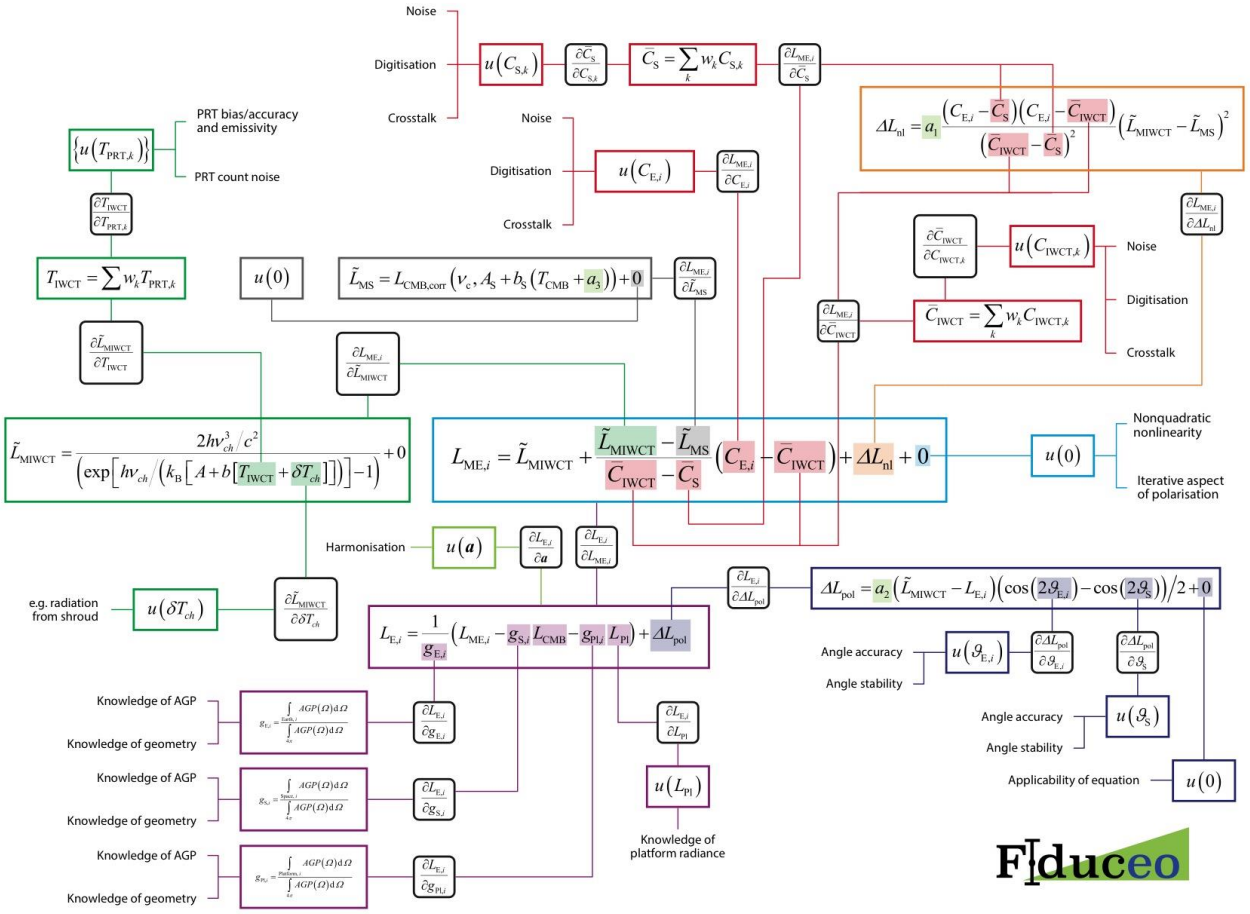

Figure 1: The Microwave Measurement function

6.2 Spectral response function

The measurement equation deals only with the photometric calibration, i. e. the conversion from counts to physical units (brightness temperature in K). For the generation of CDRs, however, it is also important to know at what frequency the brightness temperatures were measured, because otherwise the parameters characterising the line of water vapour at 183 GHz will have a systematic error, even when the photometric calibration is perfect. Models of the emission of the atmosphere like ARTS (Atmospheric Radiative Transfer Simulator) assume usually a boxcar function for the spectral response of the instrument, whose centre frequency and width are simply the specifications of the instrument in the KLM User's Guide. In the following we discuss the uncertainties of shape, width, and central frequency of the relative spectral response function (RSRF).

1. Shape: The shape of the gain transfer function was determined during ground tests of MHS on NOAA-18 and NOAA-19 (see Fig. 2). Calculating the brightness temperature to be expected in the different channels of MHS for typical atmospheres with the RSRF as determined on ground and a boxcar function gave results that differed by less than 0.1 K.

2. Width: The -3dB bandwidth of the channel H3 (LO A) as measured on ground is 460 MHz for MHS on NOAA-18 and 476 MHz for NOAA-19. The value in the KLM User's Guide is 500 MHz.
3. Central frequency: The centre frequency changes with temperature. The acceptance criteria of the ground tests were -35/+34 for H1, -92/+88 for H2, -40/+38 for H3/4, and -62/+52 for H5 (all values in MHz). These criteria were met for all channels, except for H5 (LO A) of MHS on NOAA-19, which had a frequency drift of -78 MHz at 318 K.

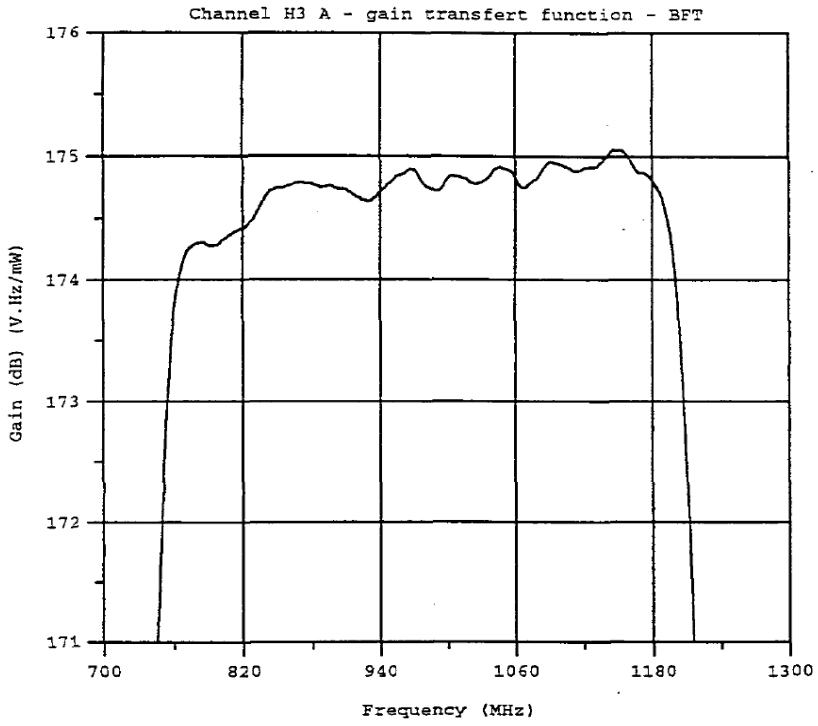

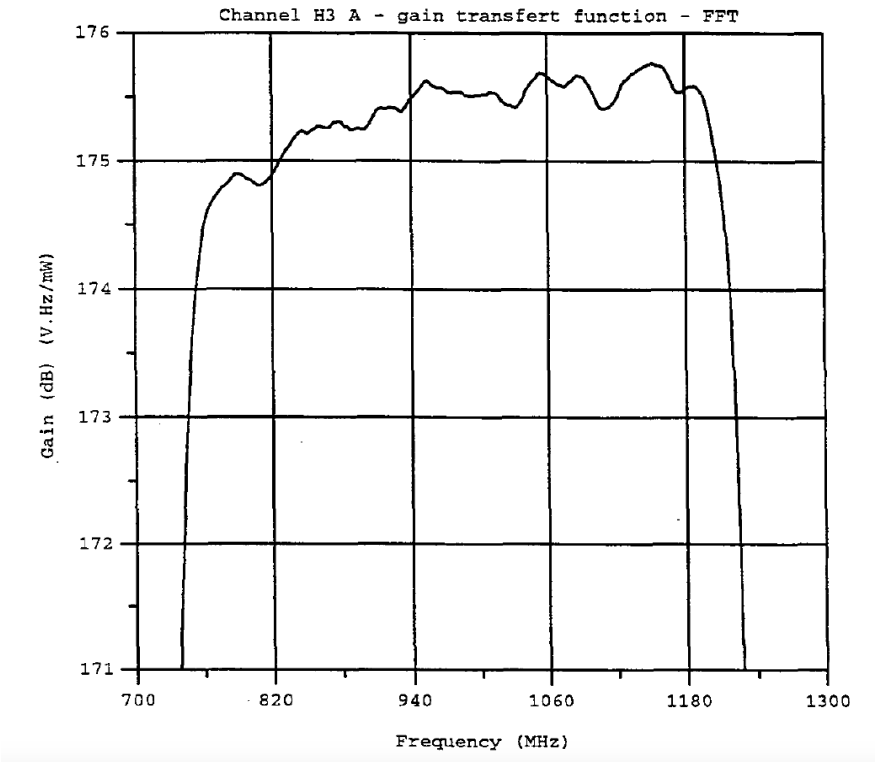

Figure 2: H3 (LO A) of MHS on NOAA-18 at 296 K (top) and NOAA-19 at 293 K (bottom).

Within the FCDR files, the SRF functions (normalized to maximum) are provided as two variables: SRF_weights, containing the weights for all frequencies that are sampled, and SRF_frequencies, containing the samples frequencies. Both variables have entries for all channels. Note that only for MHS on NOAA18 and NOAA19, the actual measured SRFs from pre-launch tests can be provided. For the other instruments, the SRFs are not known to us; hence, the variables contain fillvalues only.

6.3 Structured and independent uncertainties

6.3.1 Principles

The FIDUCEO approach to uncertainty analysis and metrological traceability is to start with the measurement function, which is the function that is used to obtain a measured output quantity value from input quantity values. The measurement function takes a general form $Y = f(X_1, X_2, \ldots, X_N) + 0$, where the output quantity Y is determined from the input quantities, the X_i. We include a "plus zero" to explicitly represent assumptions (in the form of effects expected to have zero mean) built into the form of the measurement equation.

The Guide to the Expression of Uncertainty in Measurement (GUM) describes the propagation of uncertainty through a measurement function. For this we need to consider each source of uncertainty associated with each of the input quantities and consider the error covariance between any two input quantities. We do this by considering the underlying physical effects that cause (unknown) errors in each input quantity.

For the development of an FCDR, the measurement function is that which converts raw data (e.g. measured counts and calibration target values) into the FCDR quantity (e.g. radiance or reflectance). In almost all cases, the input effects are metrologically independent (they have no common error) and the propagation of uncertainty requires only information on the magnitude of the uncertainty associated with each effect and the sensitivity coefficient that converts the uncertainty in that effect into the uncertainty associated with the FCDR measurand (e.g. radiance).

For the development of a CDR, however, the measurement function often takes as input FCDR values from different spectral bands, along with additional inputs relating to the model used. This means that we require an understanding of the error covariance between the FCDR quantities as measured in different spectral bands. Furthermore gridded, filled or smoothed products the measurement function combines data from different spatial pixels. We therefore need an understanding of the error covariance between the FCDR quantities as measured in different pixels of an image.

To account for this, the full FCDR development in FIDUCEO has included an analysis of the error correlation structure across spectral bands and across space (from pixel to pixel within a scanline and from scanline to scanline within an orbit/image). Information about this process is given in the D2-2 reports.

We are currently considering methods for sharing this information in a manageable format with CDR developers. This will include three formats: the full-FCDR, which will be useable only by experts, but which will contain all error covariance information, the easy-FCDR, which will provide some indicative error covariance information and the ensemble-FCDR which will provide multiple potential error images that can

be used in the CDR generation algorithm and which will have the error correlation form 'embedded' in the statistical generation.

For this version MW-FCDR, we provide correlation information in the correlation coefficients. Moreover, the uncertainty information is provided as three considered components: independent, structured and common (those components that have correlations structures larger than one orbit).

6.4 Included effects

Full details of all effects to be included are described in D2-2. The FCDR contains a subset of those effects.

- Uncertainty due to Earth counts noise. Estimated from the Allan deviation of the IWCT views and space views over 300 scan lines. The magnitude of the uncertainty due to Earth counts noise is equal to the value contained in the easy FCDR data variable `u_independent`.
- Uncertainty due to antenna position for earth views. The input uncertainty is estimated from the standard deviation of the position of one pixel over one orbit. Its propagated uncertainty impacts on Tb through the polarization correction term and feeds into the random uncertainty variable `u_independent`.
- Uncertainty due to noise on calibration views (IWCT and space). Estimated from the Allan Deviation of the IWCT and space view with a rolling average over 300 scan lines. This propagates into the calibration coefficients, i.e. the weighted rolling 7- scan-line average procedure is applied, and therefore is a structured effect. It is one of the components that makes up the easy FCDR data variable `u_structured`.
- Uncertainty due to reflectivity a_2 in the polarization correction. Its input uncertainty on a_2 is estimated as 100% of the values provided for the MHS on NOAA18 (in the fdf.dat file, auxiliary file for the AAPP). For other instruments, α is zero (without documentation of justification). Note that this effect has a larger correlation scale than one orbit (the same value is applied for all orbits). It is therefore part of the common effects and goes into the easy FCDR data variable `u_common`. Note that this effect will be treated in the harmonization procedure.
- Uncertainty due to antenna pattern correction of earth views. Its input uncertainty is estimated as 50% of the values for the instrument to account for the range of values for given across all instruments and channels (in the fdf.dat file) without justification for the assignment to a certain instrument and channel. It is part of the common effects and goes into the easy FCDR data variable `u_common`. Note that this effect will be treated in the harmonization procedure.
- Uncertainty due to antenna pattern correction of space views. Its input uncertainty is estimated as the standard deviation of the values given for the different space view profiles for each instrument and channels (values given in the clparams.dat file, auxiliary file for the AAPP). It is part of the common effects and goes into the easy FCDR data variable `u_common`.
- Uncertainty due to warm target correction. In this FCDR version, this effect is part of the harmonisation parameters. It is optimised in the harmonisation procedure. The uncertainty of the optimised value is given by the harmonisation. Note that only channel 3 is harmonised so far. For all other channels and MHS on NOAA-18, the input uncertainty of the warm target correction is estimated as 100% of the value for AMSUB NOAA17. All other instruments have zero, without justification (in the clparams.dat file)
  It is part of the common effects and goes into the easy FCDR data variable `u_common`.

- Uncertainty due to non-linearity. In this FCDR version, this effect is part of the harmonisation parameters. It is optimised in the harmonisation procedure. The uncertainty of the optimised value is given by the harmonisation. Note that only channel 3 is harmonised so far. For all other channels and MHS on NOAA-18, the input uncertainty of the non-linearity is estimated as 100% of the value for the instrument. It is part of the common effects and goes into the easy FCDR data variable `u_common`.
- Uncertainty due to antenna position for space views. The input uncertainty is estimated from the standard deviation of the position of one pixel over one orbit. Its propagated uncertainty impacts on Tb through the polarization correction term. Since the same averaged value for the four space view angles is used for a whole scan line of earth views, the propagated uncertainty feeds into the non-random uncertainty variable `u_structured`.
- Uncertainty due to noise of IWCT temperature measurements. Estimated from the Allan Deviation of the PRT-measured temperature of the IWCT over 300 scan lines. To the IWCT temperature, the weighted rolling average procedure is applied, and therefore its noise is a structured effect. It is one of the components that make up the easy FCDR data variable `u_structured`.
- Uncertainty due IWCT temperature measurement. The input uncertainty is assumed to be a systematic uncertainty of 0.1K for each PRT sensor. It is part of the common effects and goes into the easy FCDR data variable `u_common`.
- Uncertainty due to RFI (Radio Frequency Interference). To account for the possibility of RFI due to transmitters being switched on, we add this uncertainty to the variable `u_common` at all times when a transmitter is switched on. The quality bitmask per scanline (quality_scanline_bitmask) tells which transmitters are active. The uncertainty due to RFI is based on an estimate of the uncertainty on the applied RFI correction, reflecting an estimate of the remaining impact of RFI and of possible over-correction. The RFI impact mainly has correlation scales exceeding one orbit and is therefore included in the common effects. However, it is not constant over the whole mission as other common effects are.

Other effects, such as IWCT gradients or systematic pointing errors of the antenna are not yet included. The possibility of temperature gradients on the blackbody (the IWCT) is only flagged so far in the `data_quality_bitmask`: if a PRT-measurement is too far away from the other 4 (or 6 for AMSU-B), it will be excluded by the quality checks. However, there might be a true gradient that is not accounted for in this case. Therefore, for such cases, we set the flag “use_with_caution”, “suspect_calib_bb_temp” and “suspect_calib_prt” in the `data_quality_bitmask` to indicate that there might be an unaccounted-for error related to a temperature gradient across the IWCT.

6.5 Improvements in the calibration for a consistent FIDUCEO MW-FCDR

Revealing shortcomings or mistakes in the operational calibration (AAPP), and correcting for these as good as possible, has improved the calibration of the MW sounders to result in consistent time series. The changes and improvements in the calibration are explained in the following. Note that the significant improvements relate to the Antenna Pattern Correction and the Radio Frequency Interference. The overall improvement of the FCDR data compared to the operational data is shown in Figure 3 (see [Hans et al 2019a] for consistent time series of brightness temperature of all instruments including SSMT-2). The

obtained consistent time series for channel 3 can be used to produce a consistent CDR of upper tropospheric humidity.

6.5.1 Antenna Pattern Correction (APC)

The coefficients *g* in Eq. 6-2 to 6-4 denote the contribution from earth, space and platform to the recorded signal in the 90 earth views. The operational values for *g* are stored in the fdf.dat files of AAPP. There are certain inconsistencies within the assignment of the values, which are corrected for the FIDUCEO FCDR.

6.5.1.1 Wrong assignment to channels

For all AMSU-Bs, the assignment of *g* to the channels is wrong (all AMSU-Bs receive the same APC): channels 16 - 18 receive the correct APC, whereas channel 19 receives the APC from channel 16 and channel 20 receives the APC from channel 17. This is a clear assignment error (note that the sounding channels 18-20 share the same optical path and should therefore have the same APC).

Improvement in FCDR: The assignment is corrected such that channel 18-20 receive the APC from channel 18.

6.5.1.2 NOAA18 APC

MHS on NOAA18 receives the same APC as AMSU-B (on all NOAAs). It is suspected from bias analyses in [Hans 2018] that this causes biases.

Improvement in FCDR: As a first improvement, the APC from MHS on NOAA19 is used in the FCDR processing for MHS on NOAA18. This ensures at least that the APC considers the correct instrument type on the corresponding satellite. Investigating biases over the lifetime shows that this new assignment of NOAA19 APC to NOAA18 leads to a consistent bias reduction of all sensors with respect to the reference NOAA18.

6.5.1.3 Old APC for Metop-A

Per default value in AAPP, MHS on Metop-A receives the APC from AMSU-B (on all NOAAs). This can be changed manually to the correct APC provided by EUMETSAT in May 2007.

Improvement in FCDR: Metop-A receives its correct APC from May 2007. This reduces the bias: it is negative with respect to NOAA18 in the AAPP data. Applying the correct APC for Metop-A and the better-suited one from NOAA19 for NOAA18, reduces the bias.

6.5.2 Radio Frequency Interference (RFI)

For AMSU-B on NOAA15, it is well known that RFI has an impact on the recorded signal and hence distorts the calibrated brightness temperature (Atkinson, 2001). A correction scheme was introduced in the early years of NOAA15, but it soon became out-dated as the RFI changed erratically in these periods and the correction scheme was not updated. Consequently, NOAA15 data is contaminated with RFI that generates biases of some Kelvin with respect to NOAA18. NOAA17 was also affected by RFI although much weaker. Our analysis showed that it is highly probable that also NOAA16 and even MHS on NOAA19 are contaminated by RFI. The details are part of another paper ([Hans et al 2019b], see [Hans 2018] also).

Improvement in FCDR: In the FIDUCEO FCDR we correct for this RFI impact by a recently developed correction scheme based on global monthly mean biases against NOAA18 as function of the scan angle (the details are in [Hans et al 2019b]). The monthly mean biases reveal a stable zigzag pattern over the scan angles that can be identified as RFI (such patterns are seen for NOAA15 also). For each scan angle, and for

periods of constant RFI pattern, a correction scheme is deduced to correct for RFI impact on the earth counts. This correction scheme is based on the assumption that all change in the bias with respect to a reference month of negligible RFI contamination is assigned to RFI impact. Of course, this is not fully true due to diurnal (and hence seasonal) cycle effects that might change as the satellites drift. However, this is a small source of error for NOAA-16 and NOAA-19 since the RFI bias is much larger than the seasonal variability.

For AMSU-B on NOAA15 and NOAA17, the method needs to be modified, since both instruments do not have a month without RFI contamination in the overlapping period with the reference NOAA18. For NOAA15, we make the rough assumption that all bias against NOAA18 stems from RFI. This is not fully true, but since the RFI biases easily exceed several kelvin, it is a fair first assumption in order to try to improve the NOAA15 calibration. For NOAA17, the absolute RFI impact is much smaller. But, again, no month of significantly smaller RFI impact can be identified. Hence, we use all months of the year 2007 as reference months for the respective months of the year (in order to not completely overcorrect the seasonal cycle). However, this overcorrects the inter-annual variability to some extent, and is therefore not a perfect solution. Nonetheless, these first implementations of an RFI correction scheme are improving the consistency among the instruments.

Note that the RFI correction is deduced for the sounding channels. Due to the larger diurnal cycle impact, the method to derive the RFI correction is less suited for the other channels. However, only NOAA15 channel 2 is strongly affected by RFI. Channels 1 and 2 from the other instruments do not show strong biases due to RFI.

Applying these correction schemes within the FCDR processing to the sounding channels yields a bias reduction (see Figure 3) for AMSU-B on NOAA15, NOAA16 and NOAA17 and for MHS on NOAA19.

The correction schemes are available together with FCDR processing code. They are stored in NetCDF files per sensor (NOAA15,16,17,19).

6.5.3 Band correction

Band correction coefficients (a, b) are only provided for the black body view, although a band correction is also necessary for the DSV. This band correction for DSV should have different values for a and b.

Improvement in FCDR: The calibration in the FCDR processing uses two separate sets of band correction factors for DSV and IWCT. The new coefficients have been determined by minimising the difference of the mean of two Planck functions evaluated at the lower and higher frequency for a specific temperature and the Planck function evaluated at the central frequency for a band corrected temperature. The resulting improvement in brightness temperature is extremely small and negligible. However, it is a more consistent approach (see [Hans 2018] for details).

6.5.4 Temperature of the black body

In the AAPP processing for AMSU-B, the PRT sensors no. 6 is always excluded (weight zero). This was initiated when a constant offset of this PRT was seen in pre—launch tests. However, in later years of the instrument, our analyses did not show such a distinction of PRT no.6 with respect to the others.

Improvement in FCDR: per default, all PRT sensors are used. Individual sensors are excluded based on quality checks executed per calibration cycle [Hans 2018].

6.5.5 Temperature of the Cosmic Microwave Background

The value of the cosmic microwave background is rounded to 2.73 K in the operational processing in AAPP (see clparams.dat file of AAPP). We use the more accurate value of 2.72548 K in the FIDUCEO FCDR processing.

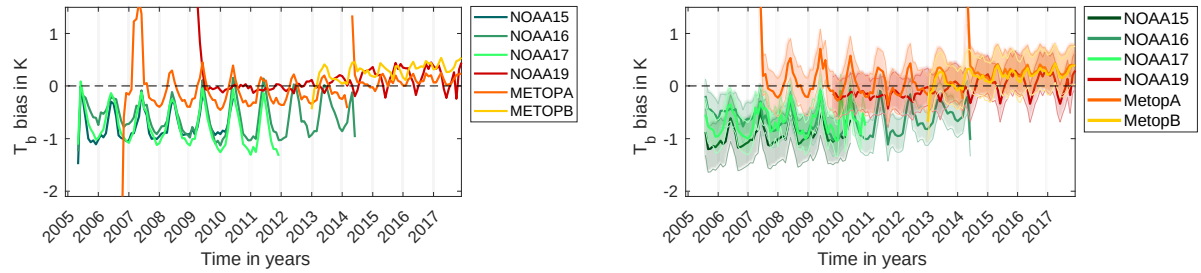

(a) Channel 1 (AAPP)

(b) Channel 1 (FCDR)

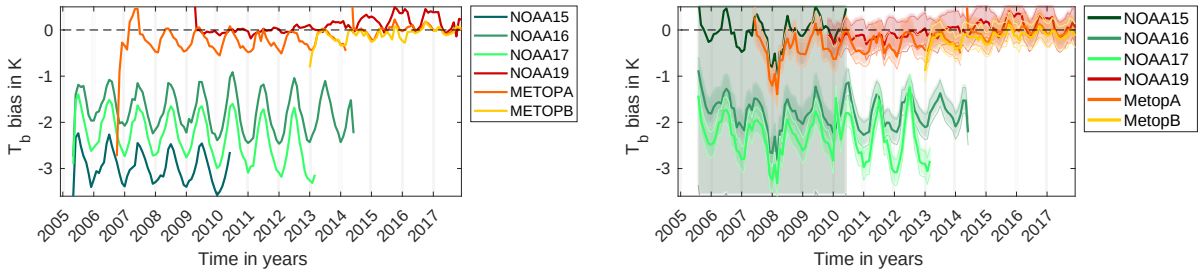

(c) Channel 2 (AAPP)

(d) Channel 2 (FCDR)

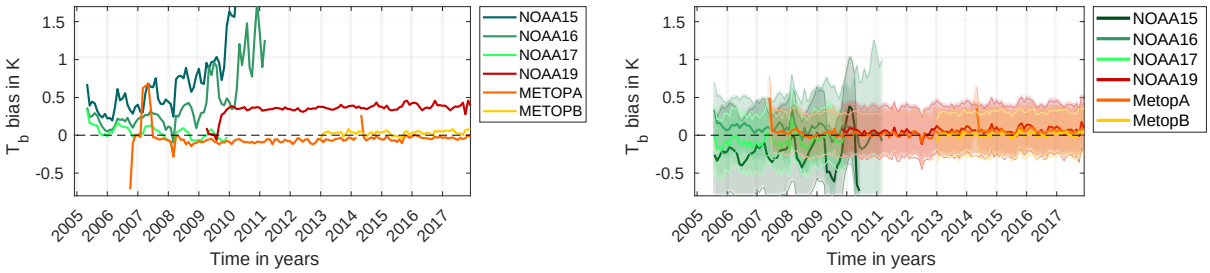

(e) Channel 3 (AAPP)

(f) Channel 3 (FCDR)

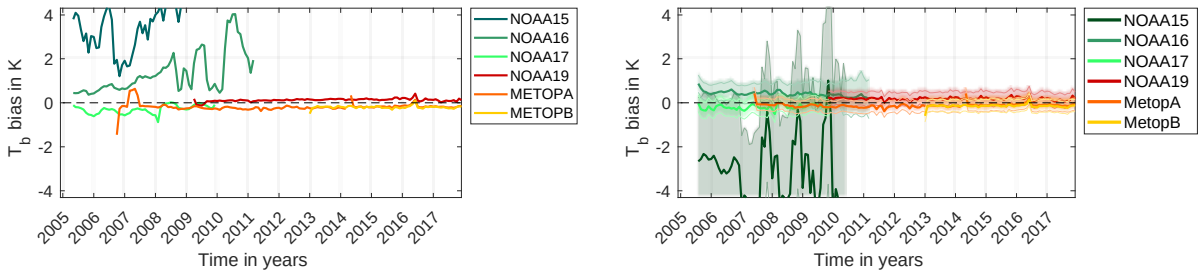

(g) Channel 4 (AAPP)

(h) Channel 4 (FCDR)

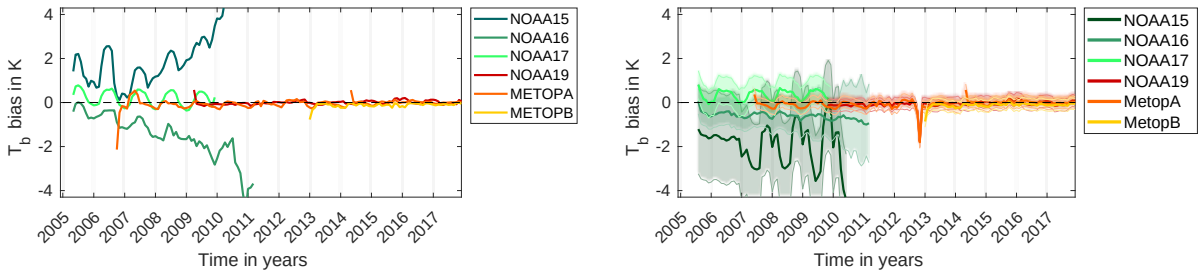

(i) Channel 5 (AAPP)

(j) Channel 5 (FCDR)

Figure 3 Comparison of inter-satellite biases (reference: MHS on NOAA-18) in operational AAPP-processed data and FIDUCEO FCDR. The shaded regions denote the uncertainties due to common effects.

6.6 Harmonisation – optimising calibration parameters

The intention is to further reduce biases by re-determining calibration parameters relating to different effects such as the polarisation correction. The origin of the parameters' values is not documented and therefore not fully trustworthy.

This re-determination of calibration parameters is carried out as an optimisation process on the training data set of matchups, aiming at a recalibration of the sensors by optimising certain calibration parameters. This is a highly complex undertaking that is not yet finished and therefore not included in the released data set version 4.1.

7 Product definition

7.1 Product contents

The L1B data were generated on-board the AMSU-B/MHS/ SSMT-2 instrument on the satellites, and subsequently processed by NOAA and archived in CLASS. The FIDUCEO team obtained the L1B data from the NOAA CLASS archive and processed it with the MATLAB software developed for MW FCDR production. The corresponding code is available at https://github.com/FIDUCEO/FCDR_MW/FCDR_processing. A detailed description of the processing chain, quality checks is provided in [Hans 2018].

In this FCDR, each file contains one orbit from equator to equator. The passing of the equator will be defined by the crossing of the equator of the "virtual nadir pixel", i.e. the latitude value corresponding to a virtual pixel located exactly at nadir between pixel 45 and 46. There are no overlaps and no gaps between adjacent orbit files (for the normal case where there is no true data gap in the l1b files). As a consequence, MW FCDR files do not correspond exactly to NOAA L1B files. Within the MW FCDR the original corresponding NOAA L1B files will be listed. Also, an indicator of the original file is given per scan line. Each MW Easy FCDR file contains:

- Basic telemetry: longitude, latitude, time, satellite zenith and azimuth angles, solar zenith and azimuth angles (the information on angles does not exist for SSMT2)
- Brightness temperatures for channels 1-5; and 16-20 resp.
- independent uncertainty information for channels 1-5; and 16-20 resp.
- structured uncertainty information for channels 1-5; and 16-20 resp.
- common uncertainties for channels 1-5; and 16-20 resp.
- 4 bitmasks indicating problems with the data. Since one of them is channel-specific, we have 3+1*5=8 variables. See section below.
- For every scan line: the original scan line number in the l1b file. This is included to ensure traceability and enable comparisons with other (older) data sets based on the l1b numbering.
- For every scan line: an indicator (0 or 1), indicating the original l1b files, which are listed in the global attributes of the NetCDF.
- Inter-channel correlation matrix for independent effects: This matrix shows the correlation coefficient between the different channels for the independent effects.
- Inter-channel correlation matrix for structured effects: This matrix shows the correlation coefficient between the different channels for the independent effects.
- Cross element correlation coefficients: Correlation coefficients per channel for correlation within a scanline (referring to structured effects)

- Cross line correlation coefficients: Correlation coefficients per channel for scanline correlation (referring to structured effects). The coefficients stem from an analysis by NPL on the correlation behaviour for data subject to rolling averages.

The data may have the following dimensions:

- x – position along the scan line, i.e. field of view or pixel.
- y – scanline number. The actual number does not necessarily correspond to the original scan line number in the corresponding l1b file, since it runs from 1 to the last line of the orbit. The original scan line number is included as separate variable.
- channel – channel number.
- delta x – distance in pixels to a specific pixel (for correlation information)
- delta y – distance in scan lines to a specific scan line (for correlation information)
- n_frequencies – number of frequencies for which the SRF is documented.

The data files contain coordinates corresponding to each of the dimensions.

7.1.1 Bit masks

There are 8 data variables that communicate quality or instrument status flags through bit masks; 5 of them are channel specific, three are valid for all channels. Global flags, valid for all channels, are stored in the quality_pixel_bitmask (valid for all channels). Channel specific issues are flagged in the quality_issue_pixel_ChX_bitmask. The second bitmask valid for all channels is data_quality_bitmask indicating sensor specific quality issues. The third bitmask valid for all channels is quality_scanline_bitmask. It contains information per scanline about the status of the transmitters. Being switched on, the transmitters may cause Radio Frequency Interference (RFI). Therefore, their status gives valuable information for possible exclusion of data, more over it triggers the u_common variable to provide uncertainty estimates on RFI.

The variable attributes define the flag meanings and their associated flag mask.

- quality_pixel_ bitmask. Set per pixel and per scanline. General bitmask available for all FIDUCEO FCDRs. Bitmask containing quality flags for (1= statement is true):

Flag Name	Bit	Description
invalid	0	General flag for invalid data. Set to TRUE if any of the following is set: invalid_input, invalid_geoloc, invalid_time, sensor_error, padded_data or any sensor specific flag that indicates invalid data.
use_with_caution	1	Input data flags set that indicate potential errors. Set to TRUE if one or more of the original sensor data flags indicate possible (but usually not critical) problems or if data in a single channel is not useable. Definition of this flag combination in sensor specific section.

invalid_input	2	Input data invalid flag. Set to TRUE if a combination of the original sensor data flags indicates unuseable data. Definition of this flag combination in sensor specific section.
invalid_geoloc	3	Flag is raised if the geolocation or viewing-geometry data of this pixel is not valid.
invalid_time	4	Flag is raised if the acquisition time data of the pixel is not valid.
sensor_error	5	Flag is raised if the measurement data or sensor status data is not valid.
padded_data	6	Pixel contains fill value or repeated data; the corresponding measurement data is stored in the previous/next orbit file. Usually this data originates from correlation-calculations overlapping orbit-file boundaries.
incomplete_channel_data	7	Flag is raised if data for one or more channels is incomplete.

- data_quality _bitmask. Set per scanline (replicated for all pixels of a scan line) . Sensor specific bitmask. Bitmask containing quality flags for (1= statement is true):

Flag Name	Bit	Description
moon_check_fails	0	The check for Moon intrusion failed. Hence no valid DSV data. If set, “invalid_input” is also set.
no_calib_bad_prt	1	All PRT measruements are bad. Usable data further away than 5 scan lines. Calibration impossible. If set, “sensor_error” is also set.
no_calib_moon_intrusion	2	Moon intrusion detected. Moon contaminates all four DSV. If set, “sensor_error” and “invalid_input” is also set.
susp_calib_bb_temp	3	Less than the full number of PRT sensors has been used for calibration. An unaccounted for temperature gradient might be missed. If set, “use_with_caution” is also set.
susp_calib_prt	4	PRT data from adjacent scan lines had to be used. OR: Less than the full number of PRT sensors has been used for calibration. OR: Fewer scan lines have been used to get the weighted average of the current one. None of those issues impacts the final calibration significantly.
susp_calib_moon_intrusion	5	Moon intrusion detected. At least one DSV could be used for calibration. If set, “use_with_caution” is also set.

- quality_issues_pixel_ChX_bitmask. For channel X, set per pixel and per scan line. Bitmask containing quality flags (1= statement is true):

Flag Name	Bit	Description
susp_calib_DSV	0	Bad DSV data for this scanline. Adjacent scanlines had to be used for calibration. OR: Less than 4 DSV could be used for calibration. This includes the case of partial Moon contamination. OR: Less than 7 scanlines have been used to get the weighted average of the current one. None of those issues impacts the final calibration significantly.

susp_calib_IWCT	1	Bad IWCT data for this scanline. Adjacent scanlines had to be used for calibration. OR: Less than 4 IWCT views could be used for calibration. OR: Less than 7 scanlines have been used to get the weighted average of the current one. None of those issues impacts the final calibration significantly.
no_calib_bad_DSV	2	Bad DSV data for this scanline. Too far away from good scanlines. Calibration impossible.
no_calib_bad_IWCT	3	Bad IWCT data for this scanline. Too far away from good scanlines. Calibration impossible.
bad_data_earthview	4	Bad data from Earth views.

- quality_scanline_bitmask. Set once per scanline. Valid across all channels. Bitmask containing quality flags (1= statement is true):

Flag Name	Bit	Description
STX1_transmitter_on	0	STX1 transmitter is on. Might cause Radio Frequency Interference. Uncertainty component u_common is increased.
STX2_transmitter_on	1	STX2 transmitter is on. Might cause Radio Frequency Interference. Uncertainty component u_common is increased.
STX3_transmitter_on	2	STX3 transmitter is on. Might cause Radio Frequency Interference. Uncertainty component u_common is increased.
STX4_transmitter_on	3	STX4 transmitter is on. Might cause Radio Frequency Interference. Uncertainty component u_common is increased.
SARR_A_transmitter_on	4	SARR-A transmitter is on. Might cause Radio Frequency Interference. Uncertainty component u_common is increased.
SARR_B_transmitter_on	5	SARR-B transmitter is on. Might cause Radio Frequency Interference. Uncertainty component u_common is increased.

Note that certain flags are not available for SSMT2 due to missing information. E.g., there is no information on possible moon-intrusions. Hence, the flags related to moon intrusions are always set to zero. The calibration is executed as if there were no moon intrusions. In fact, this is a reasonable procedure since the signal from the moon is hardly detectable in the instrument noise. Hence, its impact on the calibration will be negligible.

Also, no information on spacecraft transmitters is available for SSMT2. Consequently, the variable "quality_scanline_bitmask" only contains the fillvalue 255.

7.2 File format

Files are provided in NetCDF-4 and adhere to the CF Conventions v1.6 where possible. All data fields are internally compressed using parameters chosen based on the dynamic range of meaningful values. Filenames follow the FIDUCEO standard. The filenames have the following structure:

FIDUCEO_FCDR_L1C_{INSTRUMENT}_{SATELLITE}_{STARTTIME}_{ENDTIME}_EASY_v4.1_fv2.0.1.nc

where {INSTRUMENT} can be either AMSUB or MHS or SSMT-2. {SATELLITE} can be any of the satellites these instruments are flying on. {STARTTIME} is the date/time for the start of the orbit in UTC, with the format {YEAR}{MONTH}{DAY}{HOUR}{MINUTE}{SECOND}, {ENDTIME} is the date/time for the end of the orbit in UTC.

The rest of the filename is constant throughout the present version of the MW FCDR easy format. An example filename for AMSU-B on NOAA15 would be:

FIDUCEO_FCDR_L1C_AMSUB_NOAA15_20030101121415_20030101135524_EASY_v4.1_fv2.0.1.nc

The NetCDF format is self-documenting. Each file contains global attributes with general information, and a set of data variables. The names of data variables follow standard names from the CF Conventions for those cases where a standard name exists. Where no standard name exists, the FIDUCEO team has introduced a name not included in the standard. All data variables are stored as compressed scaled integers. Data variable attributes describe each variable and its scaling. The appendix contains an example of the headers for a particular file.

7.3 File sizes

A typical orbit file is around 7 MB for the easy FCDR (below 1MB for SSMT-2). In total, the FCDR record is about 2.2 TB.

8 Example contents

The figures below show a few examples of the contents of the FCDR.

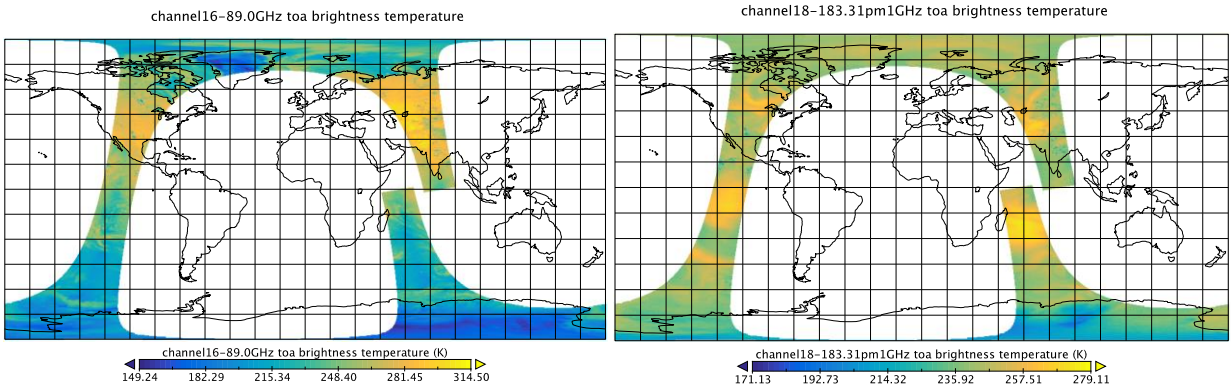

Figure 4 Content of one FCDR for the brightness temperatures for channel 16 and 18 of an orbit of AMUSB on NOAA16, 02. Aug 2007 (10:44:15 to 12:26:15).

Figure 4 shows the brightness temperature for channel 16 and 18 for a single orbit of AMSU-B on NOAA16, 02. August 2007, starting at 10:44, ending at 12:26 UTC. The brightness temperature was obtained from the calibration procedure making use of the measurement equation that is explained in the chapters above, including the improvements presented in Section 6.5. Note the Equator-To-Equator arrangement of the file that overcomes the problem of overlap between adjacent files and resulting oversampling in investigation processes.

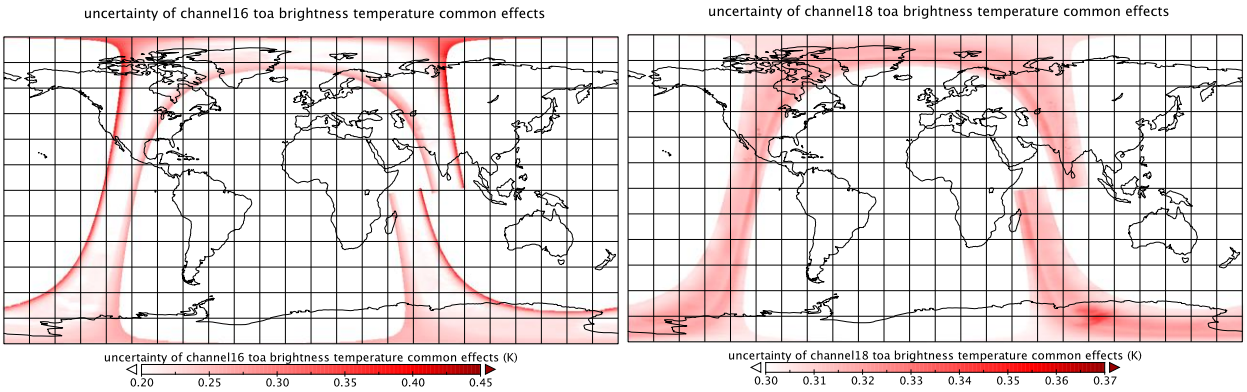

Figure 5 Uncertainty of the brightness temperature due to common effects for channel 16 and 18 for the same orbit as Figure 4.

Figure 5 shows the uncertainty on the brightness temperature due to common effects for channels 16 and 18. For channel 16, the uncertainty is strongly increased at the very (right) edge of the scan, whereas the other pixels (closer to nadir) have up to ~0.25K less uncertainty on the brightness temperature. This distinct pattern is due to the antenna pattern correction for the Earth views that attempts to correct for the non-earth radiation (i.e. from the platform and from space) entering the side-lobes of the antenna at the edge of the scan. The uncertainty on the values of this correction introduces this pattern into the final uncertainty on the brightness temperature. Since the correction is larger on the edge of the scan, the resulting absolute uncertainty on the brightness temperature is higher for these pixels. The asymmetry is based on the asymmetric correction pattern related to the viewing geometry of the instrument installed on the platform. Since no information on the uncertainty of the correction pattern is available, and since all AMSU-B instruments receive the same antenna pattern correction although their antenna patterns may differ, we assumed an uncertainty of 50% of the correction that finally leads to uncertainties of up to 0.45K. This effect dominates the overall pattern of the common uncertainties in channel 16. It is encouraging to see that even with this large uncertainty estimate of 50% of the correction, we do not generate huge and unreasonable uncertainties of the final brightness temperature.

For channel 18, we also see a scan dependent pattern in the uncertainties due to common effects, which originates from the antenna pattern correction as well. Moreover, a dependence on temperature is visible with higher uncertainty in colder regions. This is due to the polarisation correction that has a strong impact for colder temperatures. Overall, the variation of the uncertainties due to common effects in channel 18 is much smaller than for channel 16. However, the smallest uncertainty values are larger than for channel 16. This is because we include an uncertainty for the RFI-impact for channel 18 [Hans et al 2019b].. This extra uncertainty consist of a constant contribution of 0.2K accounting for a possible remaining uncorrected RFI impact and of a variable contribution correlated to the decrease in the gain of the instrument (the estimate is made on the counts and scales to brightness temperature using the measurement equation, e.g. 1 count uncertainty produces 0.1K or 1K uncertainty, depending on the gain). The variable contribution is required because of the construction of our RFI-correction. This variable contribution accounts for the possible over-correction of RFI due to diurnal cycle effects [Hans et al 2019b]. The risk for this over-correction increases as the gain decreases, since every corrected count weighs stronger with a decreased gain. Hence, we provide this variable uncertainty contribution. Consequently, in later years of NOAA16, when the gain has decreased, the uncertainty of the brightness temperature due to common effects is increased.

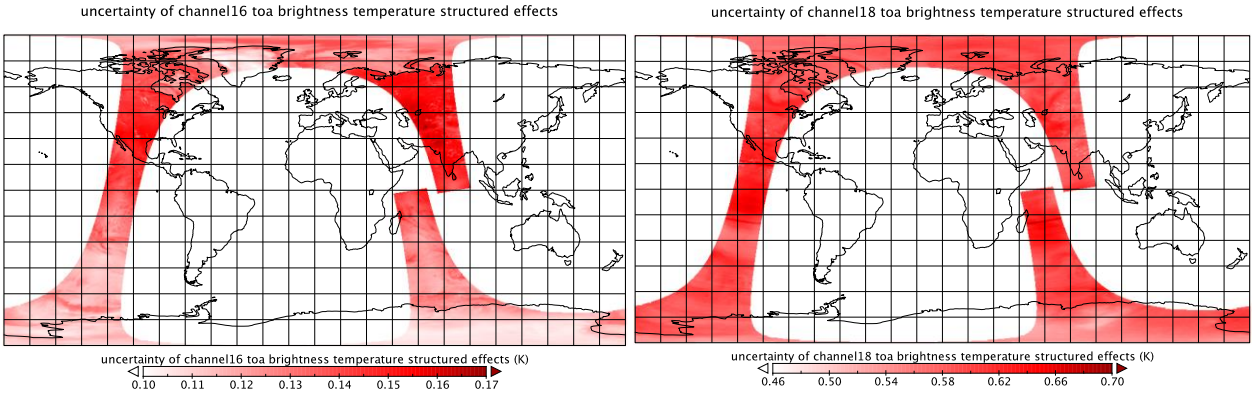

Figure 6 Uncertainty of the brightness temperature due to structured effects for channel 16 and 18 for the same orbit as Figure 4.

Figure 6 shows the same picture for the uncertainty due to structured effects. The structured effects are composed of the noise of the underlying calibration quantities, i.e. the counts of the DSV and the IWCT view as well as the noise on the PRT sensors. Additionally, the uncertainty on the viewing angle of the space view enters the overall uncertainty through the polarization correction (this correction is zero in the case of AMSU-B). Channel 16 has a smaller range of structured uncertainties and also smaller absolute values than channel 18.

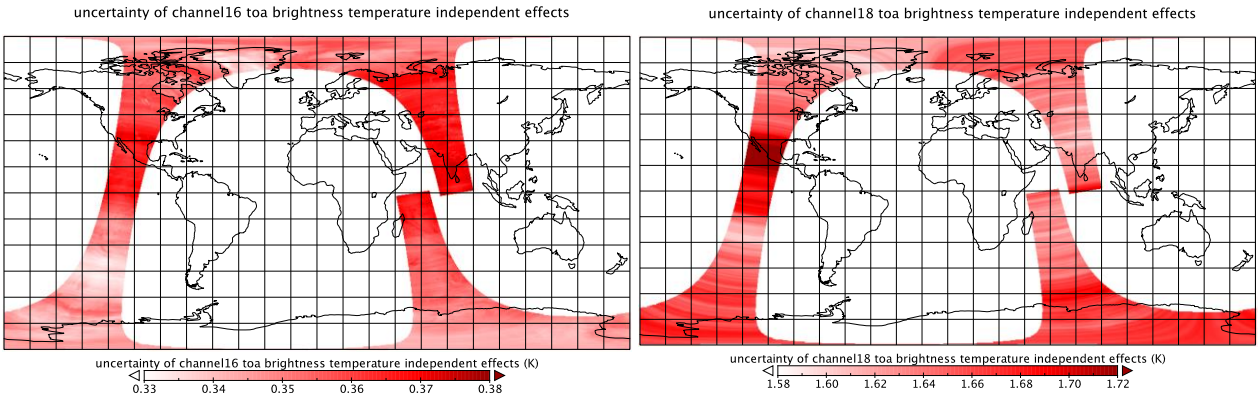

Figure 7 Uncertainty of the brightness temperature due to independent effects for channel 16 and 18 for the same orbit as Figure 4

Figure 7 shows the same picture for the uncertainty due to independent effects. This includes the independent uncertainty due to the position of the earth views that impacts on the polarization correction independently for each pixel and hence enters the uncertainty due to independent effects. Note however, that the polarization correction is zero for AMSU-B and has therefore no effect in this example. This is different for MHS, but the impact of this effect is very. The dominating effect for the independent part is the noise on the earth counts for both MHS an AMSU-B. It is estimated for each (rolling) window of 300 scan lines by the Allan deviation (the detailed procedure is described in [Hans et al 2017]). Note that the ranges of uncertainty especially due to independent effects are quite different for channel 16 and 18. Compared to the uncertainty due to structured effects, the uncertainty due to independent effects is much larger for channel 18. This is also visible in the histogram of structured and independent uncertainties shown below.

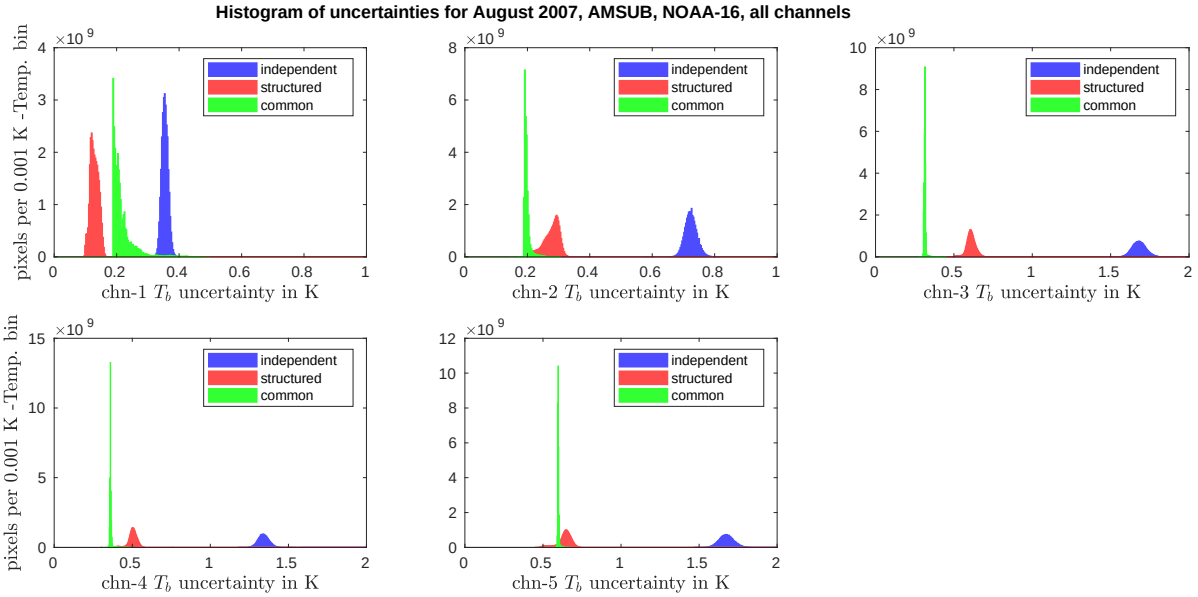

Figure 8 Histogram of uncertainties due to independent, structured and common effects for the whole month of August 2007 of NOAA16 AMSUB data for all channels.

Figure 8 shows the histogram of uncertainties for AMSU-B on NOAA15 in August 2007. For each channel, the distribution of uncertainties on the brightness temperatures due to independent (blue), structured (red) and common (green) effects is displayed. For all channels, the uncertainty due to independent effects strongly dominates the overall uncertainty budget. This effect is most significant for channel 18, where the peaks of the distributions are at about 0.3 K (common), 0.6 K (structured) and 1.7 K (independent, i.e. the noise on earth counts).

A. Example header

The extract below shows the header for the FIDUCEO FCDR L1C file of NOAA-16, AMSUB, containing data starting at 02-08-2007 10:44:15 UTC, ending at 02-08-2007 12:26:15, data version 4.1, format version 2.0.1. This corresponds to a single full orbit going from equator-to-equator.

```
netcdf
file:/Users/u237015/t7home/ihans/xchange/FIDUCEO_FCDR_L1C_AMSUB_NOAA16_20070802104415_20070802122615
_EASY_v4.0_fv2.0.1.nc {
   dimensions:
     x = 90;
     y = UNLIMITED;   // (2302 currently)
     channel = 5;
     delta_y = 7;
     delta_x = 90;
     n_frequency = 63;
   variables:
     short latitude(y=2302, x=90);
       :standard_name = "latitude";
       :long_name = "latitude";
       :units = "degree north";
       :scale_factor = 0.01; // double
       :description = "Latitude for each pixel in every scanline.";
       :_FillValue = -32768S; // short
       :_ChunkSizes = 100, 90; // int

     short longitude(y=2302, x=90);
```

```
  :standard_name = "longitude";
  :long_name = "longitude";
  :units = "degree east";
  :scale_factor = 0.01; // double
  :description = "Longitude for each pixel in every scanline.";
  :_FillValue = -32768S; // short
  :_ChunkSizes = 100, 90; // int

int Satellite_azimuth_angle(y=2302, x=90);
  :_FillValue = -2147483648; // int
  :long_name = "Satellite_azimuth_angle";
  :standard_name = "sensor_azimuth_angle";
  :coordinates = "latitude longitude";
  :units = "degree";
  :scale_factor = 0.01; // double
  :description = "Satellite azimuth angle for each view (x) in every scanline (y).";
  :_ChunkSizes = 100, 90; // int

int Satellite_zenith_angle(y=2302, x=90);
  :_FillValue = -2147483648; // int
  :long_name = "Satellite_zenith_angle";
  :standard_name = "sensor_zenith_angle";
  :coordinates = "latitude longitude";
  :units = "degree";
  :scale_factor = 0.01; // double
  :description = "Satellite zenith angle for each view (x) in every scanline (y).";
  :_ChunkSizes = 100, 90; // int

int Solar_azimuth_angle(y=2302, x=90);
  :_FillValue = -2147483648; // int
  :standard_name = "solar_azimuth_angle";
  :long_name = "Solar_azimuth_angle";
  :coordinates = "latitude longitude";
  :units = "degree";
  :scale_factor = 0.01; // double
  :description = "Solar azimuth angle for each view (x) in every scanline (y).";
  :_ChunkSizes = 100, 90; // int

int Solar_zenith_angle(y=2302, x=90);
  :_FillValue = -2147483648; // int
  :standard_name = "solar_zenith_angle";
  :long_name = "Solar_zenith_angle";
  :coordinates = "latitude longitude";
  :units = "degree";
  :scale_factor = 0.01; // double
  :description = "Solar zenith angle for each each view (x) in every scanline (y).";
  :_ChunkSizes = 100, 90; // int

short Ch16_BT(y=2302, x=90);
  :standard_name = "toa_brightness_temperature";
  :long_name = "channel16-89.0GHz_toa_brightness_temperature";
  :coordinates = "latitude longitude";
  :units = "K";
  :scale_factor = 0.01; // double
  :description = "channel 16 brightness temperature per view (x) and scanline (y)";
  :_FillValue = -1US; // short
  :_Unsigned = "true";
  :_ChunkSizes = 100, 90; // int

short Ch17_BT(y=2302, x=90);
  :standard_name = "toa_brightness_temperature";
  :long_name = "channel17-150.0GHz_toa_brightness_temperature";
  :coordinates = "latitude longitude";
  :units = "K";
  :scale_factor = 0.01; // double
  :description = "channel 17 brightness temperature per view (x) and scanline (y)";
  :_FillValue = -1US; // short
  :_Unsigned = "true";
  :_ChunkSizes = 100, 90; // int

short Ch18_BT(y=2302, x=90);
  :standard_name = "toa_brightness_temperature";
  :long_name = "channel18-183.31pm1GHz_toa_brightness_temperature";
  :coordinates = "latitude longitude";
  :units = "K";
  :scale_factor = 0.01; // double
  :description = "channel 18 brightness temperature per view (x) and scanline (y)";
```

```
        :_FillValue = -1US; // short
        :_Unsigned = "true";
        :_ChunkSizes = 100, 90; // int

      short Ch19_BT(y=2302, x=90);
        :standard_name = "toa_brightness_temperature";
        :long_name = "channel19-183.31pm3GHz_toa_brightness_temperature";
        :coordinates = "latitude longitude";
        :units = "K";
        :scale_factor = 0.01; // double
        :description = "channel 19 brightness temperature per view (x) and scanline (y)";
        :_FillValue = -1US; // short
        :_Unsigned = "true";
        :_ChunkSizes = 100, 90; // int

      short Ch20_BT(y=2302, x=90);
        :standard_name = "toa_brightness_temperature";
        :long_name = "channel20-183.31pm7GHz_toa_brightness_temperature";
        :coordinates = "latitude longitude";
        :units = "K";
        :scale_factor = 0.01; // double
        :description = "channel 20 brightness temperature per view (x) and scanline (y)";
        :_FillValue = -1US; // short
        :_Unsigned = "true";
        :_ChunkSizes = 100, 90; // int

      short quality_pixel_bitmask(y=2302, x=90);
        :standard_name = "status_flag";
        :coordinates = "latitude longitude";
        :long_name = "Bitmask for quality per pixel";
        :flag_masks = "1, 2, 4, 8, 16, 32, 64, 128";
        :flag_meanings = "invalid use_with_caution invalid_input invalid_geoloc invalid_time
sensor_error padded_data incomplete_channel_data ";
        :_FillValue = 255US; // short
        :_Unsigned = "true";
        :_ChunkSizes = 100, 90; // int

      short data_quality_bitmask(y=2302, x=90);
        :standard_name = "status_flag";
        :coordinates = "latitude longitude";
        :long_name = "Sensor specific bitmask for quality per pixel";
        :flag_masks = "1, 2, 4, 8, 16, 32";
        :flag_meanings = "moon_check_fails no_calib_bad_prt no_calib_moon_intrusion
susp_calib_bb_temp susp_calib_prt susp_calib_moon_intrusion ";
        :_FillValue = 255US; // short
        :_Unsigned = "true";
        :_ChunkSizes = 100, 90; // int

      byte quality_scanline_bitmask(y=2302);
        :standard_name = "status_flag";
        :long_name = "Bitmask for quality per scanline";
        :flag_masks = "1, 2, 4, 8, 16, 32";
        :flag_meanings = "STX1_transmitter_on STX2_transmitter_on STX3_transmitter_on
STX4_transmitter_on SARR_A_transmitter_on SARR_B_transmitter_on";
        :_FillValue = -1UB; // byte
        :_Unsigned = "true";
        :_ChunkSizes = 100; // int

      byte quality_issue_pixel_Ch16_bitmask(y=2302, x=90);
        :standard_name = "status_flag";
        :long_name = "Bitmask for quality issues in Ch16 per pixel";
        :coordinates = "latitude longitude";
        :flag_masks = "1,2,4,8,16";
        :flag_meanings = "susp_calib_DSV susp_calib_IWCT no_calib_bad_DSV no_calib_bad_IWCT
bad_data_earthview";
        :_FillValue = -1UB; // byte
        :_Unsigned = "true";
        :_ChunkSizes = 100, 90; // int

      byte quality_issue_pixel_Ch17_bitmask(y=2302, x=90);
        :standard_name = "status_flag";
        :long_name = "Bitmask for quality issues in Ch17 per pixel";
        :coordinates = "latitude longitude";
        :flag_masks = "1,2,4,8,16";
        :flag_meanings = "susp_calib_DSV susp_calib_IWCT no_calib_bad_DSV no_calib_bad_IWCT
bad_data_earthview";
        :_FillValue = -1UB; // byte
```

```
        :_Unsigned = "true";
        :_ChunkSizes = 100, 90; // int

      byte quality_issue_pixel_Ch18_bitmask(y=2302, x=90);
        :standard_name = "status_flag";
        :long_name = "Bitmask for quality issues in Ch18 per pixel";
        :coordinates = "latitude longitude";
        :flag_masks = "1,2,4,8,16";
        :flag_meanings = "susp_calib_DSV susp_calib_IWCT no_calib_bad_DSV no_calib_bad_IWCT
bad_data_earthview";
        :_FillValue = -1UB; // byte
        :_Unsigned = "true";
        :_ChunkSizes = 100, 90; // int

      byte quality_issue_pixel_Ch19_bitmask(y=2302, x=90);
        :standard_name = "status_flag";
        :long_name = "Bitmask for quality issues in Ch19 per pixel";
        :coordinates = "latitude longitude";
        :flag_masks = "1,2,4,8,16";
        :flag_meanings = "susp_calib_DSV susp_calib_IWCT no_calib_bad_DSV no_calib_bad_IWCT
bad_data_earthview";
        :_FillValue = -1UB; // byte
        :_Unsigned = "true";
        :_ChunkSizes = 100, 90; // int

      byte quality_issue_pixel_Ch20_bitmask(y=2302, x=90);
        :standard_name = "status_flag";
        :long_name = "Bitmask for quality issues in Ch20 per pixel";
        :coordinates = "latitude longitude";
        :flag_masks = "1,2,4,8,16";
        :flag_meanings = "susp_calib_DSV susp_calib_IWCT no_calib_bad_DSV no_calib_bad_IWCT
bad_data_earthview";
        :_FillValue = -1UB; // byte
        :_Unsigned = "true";
        :_ChunkSizes = 100, 90; // int

      int Time(y=2302);
        :long_name = "Time_of_Scan_line";
        :units = "s";
        :description = "Acquisition time of the scan line in seconds since 1970-01-01 00:00:00.";
        :_FillValue = -2147483648; // int
        :_ChunkSizes = 100; // int

      short scanline_origl1b(y=2302);
        :long_name = "Original_Scan_line_number";
        :description = "Original scan line numbers from corresponding l1b records.";
        :_FillValue = -32768S; // short
        :_ChunkSizes = 100; // int

      byte scanline_map_to_origl1bfile(y=2302);
        :long_name = "Indicator of original file";
        :description = "Indicator for mapping each line to its corresponding original level 1b
file.\\nSee global attribute \"source\" for the filenames. 0 corresponds to 1st listed file, 1 to
2nd file.";
        :_FillValue = -1UB; // byte
        :_Unsigned = "true";
        :_ChunkSizes = 100; // int

      short channel_correlation_matrix_independent(channel=5, channel=5);
        :long_name = "Channel_error_correlation_matrix_independent_effects";
        :units = "1";
        :scale_factor = 0.01; // double
        :description = "Cross-Channel error correlation matrix for independent effects. ";
        :_FillValue = -32768S; // short
        :_ChunkSizes = 5, 5; // int

      short channel_correlation_matrix_structured(channel=5, channel=5);
        :_FillValue = -32768S; // short
        :long_name = "Channel_error_correlation_matrix_structured_effects";
        :units = "1";
        :scale_factor = 0.01; // double
        :description = "Cross-Channel error correlation matrix for structured effects. ";
        :_ChunkSizes = 5, 5; // int

      short channel_correlation_matrix_common(channel=5, channel=5);
        :long_name = "Channel_error_correlation_matrix_common_effects";
        :units = "1";
```

```
    :scale_factor = 0.01; // double
    :description = "Cross-Channel error correlation matrix for common effects.";
    :_FillValue = -32768S; // short
    :_ChunkSizes = 5, 5; // int

  short cross_line_correlation_coefficients(delta_y=7, channel=5);
    :long_name = "cross_line_correlation_coefficients";
    :units = "1";
    :scale_factor = 1.0E-4; // double
    :description = "Correlation coefficients per channel for scanline correlation. Note that this
is a rough estimation as only the structured effects are taken into account. The correlation for the
independent effects is zero by definition and the correlation for the common effects is 1 for all
scan lines and orbits.";
    :_FillValue = -1US; // short
    :_Unsigned = "true";
    :_ChunkSizes = 7, 5; // int

  short cross_element_correlation_coefficients(delta_x=90, channel=5);
    :long_name = "cross_element_correlation_coefficients";
    :units = "1";
    :scale_factor = 0.01; // double
    :description = "Correlation coefficients per channel for correlation within a scanline. Note
that this is a rough estimation as only the structured effects are taken into account. The
correlation for the independent effects is zero by definition and the correlation for the common
effects is probably variable within one scan line.";
    :_FillValue = -1US; // short
    :_Unsigned = "true";
    :_ChunkSizes = 90, 5; // int

  int SRF_frequencies(channel=5, n_frequency=63);
    :_FillValue = -2147483648; // int
    :long_name = "Spectral Response Function frequencies";
    :units = "MHz";
    :scale_factor = 0.01; // double
    :description = "Per channel: frequencies for the relative spectral response function.";
    :_ChunkSizes = 5, 63; // int

  short SRF_weights(channel=5, n_frequency=63);
    :long_name = "Spectral Response Function weights";
    :units = "dB";
    :scale_factor = 0.001; // double
    :description = "Per channel: weights for the relative spectral response function.";
    :_FillValue = -32768S; // short
    :_ChunkSizes = 5, 63; // int

  short u_independent_Ch16_BT(y=2302, x=90);
    :long_name = "uncertainty_of_channel16_toa_brightness_temperature_independent_effects";
    :coordinates = "latitude longitude";
    :units = "K";
    :scale_factor = 1.0E-4; // double
    :description = "Uncertainty of the TOA brightness temperature. Contains all considered
independent effects of uncertainty.";
    :_FillValue = -1US; // short
    :_Unsigned = "true";
    :_ChunkSizes = 100, 90; // int

  short u_independent_Ch17_BT(y=2302, x=90);
    :long_name = "uncertainty_of_channel17_toa_brightness_temperature_independent_effects";
    :coordinates = "latitude longitude";
    :units = "K";
    :scale_factor = 1.0E-4; // double
    :description = "Uncertainty of the TOA brightness temperature. Contains all considered
independent effects of uncertainty.";
    :_FillValue = -1US; // short
    :_Unsigned = "true";
    :_ChunkSizes = 100, 90; // int

  short u_independent_Ch18_BT(y=2302, x=90);
    :long_name = "uncertainty_of_channel18_toa_brightness_temperature_independent_effects";
    :coordinates = "latitude longitude";
    :units = "K";
    :scale_factor = 1.0E-4; // double
    :description = "Uncertainty of the TOA brightness temperature. Contains all considered
independent effects of uncertainty.";
    :_FillValue = -1US; // short
    :_Unsigned = "true";
    :_ChunkSizes = 100, 90; // int
```

```
     short u_independent_Ch19_BT(y=2302, x=90);
       :_FillValue = -1US; // short
       :long_name = "uncertainty_of_channel19_toa_brightness_temperature_independent_effects";
       :coordinates = "latitude longitude";
       :units = "K";
       :scale_factor = 1.0E-4; // double
       :description = "Uncertainty of the TOA brightness temperature. Contains all considered
independent effects of uncertainty.";
       :_Unsigned = "true";
       :_ChunkSizes = 100, 90; // int

     short u_independent_Ch20_BT(y=2302, x=90);
       :long_name = "uncertainty_of_channel20_toa_brightness_temperature_independent_effects";
       :coordinates = "latitude longitude";
       :units = "K";
       :scale_factor = 1.0E-4; // double
       :description = "Uncertainty of the TOA brightness temperature. Contains all considered
independent effects of uncertainty.";
       :_FillValue = -1US; // short
       :_Unsigned = "true";
       :_ChunkSizes = 100, 90; // int

     short u_structured_Ch16_BT(y=2302, x=90);
       :long_name = "uncertainty_of_channel16_toa_brightness_temperature_structured_effects";
       :coordinates = "latitude longitude";
       :units = "K";
       :scale_factor = 1.0E-4; // double
       :description = "Uncertainty of the TOA brightness temperature. Contains all considered
structured effects of uncertainty.";
       :_FillValue = -1US; // short
       :_Unsigned = "true";
       :_ChunkSizes = 100, 90; // int

     short u_structured_Ch17_BT(y=2302, x=90);
       :long_name = "uncertainty_of_channel17_toa_brightness_temperature_structured_effects";
       :coordinates = "latitude longitude";
       :units = "K";
       :scale_factor = 1.0E-4; // double
       :description = "Uncertainty of the TOA brightness temperature. Contains all considered
structured effects of uncertainty.";
       :_FillValue = -1US; // short
       :_Unsigned = "true";
       :_ChunkSizes = 100, 90; // int

     short u_structured_Ch18_BT(y=2302, x=90);
       :long_name = "uncertainty_of_channel18_toa_brightness_temperature_structured_effects";
       :coordinates = "latitude longitude";
       :units = "K";
       :scale_factor = 1.0E-4; // double
       :description = "Uncertainty of the TOA brightness temperature. Contains all considered
structured effects of uncertainty.";
       :_FillValue = -1US; // short
       :_Unsigned = "true";
       :_ChunkSizes = 100, 90; // int

     short u_structured_Ch19_BT(y=2302, x=90);
       :long_name = "uncertainty_of_channel19_toa_brightness_temperature_structured_effects";
       :coordinates = "latitude longitude";
       :units = "K";
       :scale_factor = 1.0E-4; // double
       :description = "Uncertainty of the TOA brightness temperature. Contains all considered
structured effects of uncertainty.";
       :_FillValue = -1US; // short
       :_Unsigned = "true";
       :_ChunkSizes = 100, 90; // int

     short u_structured_Ch20_BT(y=2302, x=90);
       :long_name = "uncertainty_of_channel20_toa_brightness_temperature_structured_effects";
       :coordinates = "latitude longitude";
       :units = "K";
       :scale_factor = 1.0E-4; // double
       :description = "Uncertainty of the TOA brightness temperature. Contains all considered
structured effects of uncertainty.";
       :_FillValue = -1US; // short
       :_Unsigned = "true";
       :_ChunkSizes = 100, 90; // int
```

```
     int u_common_Ch16_BT(y=2302, x=90);
       :_FillValue = -1U; // int
       :long_name = "uncertainty_of_channel16_toa_brightness_temperature_common_effects";
       :coordinates = "latitude longitude";
       :units = "K";
       :scale_factor = 1.0E-4; // double
       :description = "Uncertainty of the TOA brightness temperature. Contains all considered common
effects of uncertainty.";
       :_Unsigned = "true";
       :_ChunkSizes = 100, 90; // int

     int u_common_Ch17_BT(y=2302, x=90);
       :long_name = "uncertainty_of_channel17_toa_brightness_temperature_common_effects";
       :coordinates = "latitude longitude";
       :units = "K";
       :scale_factor = 1.0E-4; // double
       :description = "Uncertainty of the TOA brightness temperature. Contains all considered common
effects of uncertainty.";
       :_FillValue = -1U; // int
       :_Unsigned = "true";
       :_ChunkSizes = 100, 90; // int

     int u_common_Ch18_BT(y=2302, x=90);
       :long_name = "uncertainty_of_channel18_toa_brightness_temperature_common_effects";
       :coordinates = "latitude longitude";
       :units = "K";
       :scale_factor = 1.0E-4; // double
       :description = "Uncertainty of the TOA brightness temperature. Contains all considered common
effects of uncertainty.";
       :_FillValue = -1U; // int
       :_Unsigned = "true";
       :_ChunkSizes = 100, 90; // int

     int u_common_Ch19_BT(y=2302, x=90);
       :long_name = "uncertainty_of_channel19_toa_brightness_temperature_common_effects";
       :coordinates = "latitude longitude";
       :units = "K";
       :scale_factor = 1.0E-4; // double
       :description = "Uncertainty of the TOA brightness temperature. Contains all considered common
effects of uncertainty.";
       :_FillValue = -1U; // int
       :_Unsigned = "true";
       :_ChunkSizes = 100, 90; // int

     int u_common_Ch20_BT(y=2302, x=90);
       :long_name = "uncertainty_of_channel20_toa_brightness_temperature_common_effects";
       :coordinates = "latitude longitude";
       :units = "K";
       :scale_factor = 1.0E-4; // double
       :description = "Uncertainty of the TOA brightness temperature. Contains all considered common
effects of uncertainty.";
       :_FillValue = -1U; // int
       :_Unsigned = "true";
       :_ChunkSizes = 100, 90; // int

   // global attributes:
   :Conventions = "CF-1.6";
   :institution = "Universitaet Hamburg";
   :source = "NSS.AMBX.NL.D07214.S0936.E1131.B3536364.GC.gz
NSS.AMBX.NL.D07214.S1126.E1251.B3536465.GC.gz ";
   :title = "Microwave humidity sounder Easy-Fundamental Climate Data Record (MW-Easy-FCDR)";
   :history = ; // double
   :references = ; // double
   :id = "product doi will be placed here";
   :naming_authority = "Institution that published the doi";
   :licence = "This dataset is released for use under CC-BY licence
(https://creativecommons.org/licenses/by/4.0/) and was developed in the EC \\nFIDUCEO project
Fidelity and Uncertainty in Climate Data Records from Earth Observations. Grant Agreement: 638822.";
   :writer_version = "MATLAB script write_easyFCDR_orbitfile_AMSUB.m";
   :satellite = "noaa16";
   :instrument = "amsub";
   :comment = "This version is based on consistent, improved calibration (see Product User Guide
v4.1).";
   :StartTimeOfOrbit = "02-Aug-2007 10:44:15";
   :EndTimeOfOrbit = "02-Aug-2007 12:26:15";
 }
```

B. Future plans

- Investigation of possible further improvements (increasing consistency) with harmonisation

C. Known problems

1. The SSMT2 instruments cannot compete with the quality of the MHS and AMSU-B instruments, because the antenna pattern correction for SSMT2 is completely unknown such that only antenna temperatures can be provided instead of brightness temperatures.

2. The RFI-correction for NOAA15 and NOAA17 is imperfect. This is mostly relevant for NOAA15, showing larger deviations from the other instruments. The imperfection is due to a lack of uncontaminated data. This lack prohibits the clean derivation and application of our RFI-correction scheme. The imperfection results in insufficient correction or over-correction.

3. The RFI-correction method does not work for the surface channels due to strong diurnal cycle impact. Hence, the surface channels at 89 GHz and 150 GHz cannot be RFI-corrected. This affects NOAA15 most, because channel 17 (150 GHz) was strongly influenced by RFI.

4. There is no knowledge of RFI on SSMT-2, but we cannot rule out that RFI exists also for this instrument.

5. Some bad values may not be captured by the quality bitmasks. Hence, it is recommended to additionally filter all fillvalues.